
Numerical Modeling of Gob and Container Forming

Matthew Hyre – Yves Rubin

Virginia Military Institute
Lexington, VA 24450 USA
mrhyre@mail.vmi.edu

Polyflow s.a.
16 Place de l'Université
B-1348 Louvain-la-Neuve, Belgium
Rubin@mss.isunet.edu

ABSTRACT: Recent advances in numerical simulation capabilities have made the modeling of both glass conditioning and forming processes feasible. Glass forming operations include large free surface deformations, conjugate heat transfer, and complex contact phenomena. In this paper, glass container forming processes are modeled to provide insight into the impacts of the various stages of forming and conditioning on final container quality. The numerical model utilizes finite elements and includes the effects of viscoelasticity, surface tension, and time varying heat transfer. Special attention is given to areas that require further developments in numerical capabilities and an increased knowledge of boundary conditions and material properties.

KEY WORDS: container forming, computational modeling, finite element

1. Introduction

Industrial container glass forming is a complex sequence of unit processes that includes melting and refining the raw material, cooling and conditioning the molten glass in forehearth, and the actual forming processes in the IS machine. The sensitivity of glass to the processing history requires that comprehensive modeling be used to yield accurate design information in order to control thermal gradients and stress distributions throughout the forming process.

To demonstrate how thermal problems in gob forming equipment can affect the consistency of final container quality, a numerical investigation was carried out on the flow and thermal conditions of molten glass during its passage through a container forming IS machine. In addition to specific thermo-mechanical coupling capabilities,

'mesh-to-mesh' interpolation, mesh superposition, and remeshing techniques were used to allow a continuation of the calculations in spite of very severe mesh deformations.

2. Governing Equations

For an incompressible fluid, the Cauchy stress tensor \mathbf{s} is determined up to an arbitrary isotropic tensor [CRO 82]:

$$\mathbf{s} = -p\mathbf{I} + \mathbf{T} \quad [1]$$

where p is the pressure, \mathbf{I} is the unit tensor, and \mathbf{T} is the extra stress tensor. Conservation of mass for an incompressible fluid yields is used as a kinematic constraint imposed on the possible motions of the fluid.

Conservation of linear momentum gives:

$$\nabla \cdot \mathbf{s} + \mathbf{r}\mathbf{f} = \mathbf{r} \frac{D\mathbf{v}}{Dt} \quad [2]$$

where the operator D/Dt is the material time derivative. Finally the energy equation for an incompressible fluid reads:

$$\mathbf{r}C(T) \frac{DT}{Dt} = \mathbf{T} : \nabla \mathbf{v} + \mathbf{r} - \nabla \cdot \mathbf{q} \quad [3]$$

where C is the heat capacity, \mathbf{r} is the volumetric heat source, and \mathbf{q} is the heat flux. Viscous heating can enter through the term $\mathbf{T} : \nabla \mathbf{v}$.

3. Modeling Glass Flow in the Body of the Container

For most regions of the glass forming domain, the glass was modeled as a generalized Newtonian fluid. In this case, the extra-stress tensor is:

$$\mathbf{T} = 2\mathbf{h}(\dot{\mathbf{g}}, T)\mathbf{D} \quad [4]$$

where \mathbf{D} is the rate of deformation and η is the shear viscosity which varies with temperature and shear rate, $\dot{\mathbf{g}}$. The non-Newtonian behavior of glass due to shear thinning was characterized using the data of Simmons *et al.* [SIM 82,88, 90].

The Williams-Landel-Ferry [WIL 55] equation was used to describe the variation of viscosity with temperature, $\mathbf{h}(T, \dot{\mathbf{g}}) = H(T)\mathbf{h}(\dot{\mathbf{g}})$:

$$\ln(H(T)) = \frac{c_1(T_r - T_a)}{c_2 + T_r - T_a} - \frac{c_1(T - T_a)}{c_2 + T - T_a} \quad [5]$$

where c_1 and c_2 are the WLF constants, and T_r and T_a are reference temperatures. For the glass under investigation the values of these constants were 20.93, 161.05 K, 797.96 K, and 2673.93 K respectively. The WLF model fit the experimental viscosity data better than an Arrhenius law for a wider range of temperatures, especially close to the glass transition temperature.

4. Modeling the Glass in the Neckring

The generalized Newtonian fluid model is unable to describe viscoelastic phenomena related to normal stresses and stress relaxation. These phenomena begin to become important as the glass cools near the mold temperatures. During the formation of the parison, viscoelastic effects (as well as shear thinning effects) become important as the glass fills the neckring. The extra-stress tensor was broken down into two components, the viscoelastic contribution, \mathbf{T}_1 , and a purely viscous contribution, \mathbf{T}_2 .

The viscous component of the extra-stress is given by:

$$\mathbf{T}_2 = 2\mathbf{h}_2(\dot{\mathbf{g}}, T)\mathbf{D} \quad [5]$$

The viscoelastic component was developed from typical differential models used in numerical simulations:

$$\mathbf{A}(\mathbf{T}_1, I) \cdot \mathbf{T}_1 + I(\dot{\mathbf{g}}, T)\mathbf{D} \quad [6]$$

Here, λ is the relaxation time, η_1 is a viscosity coefficient; both are functions of shear rate and temperature. \mathbf{A} denotes a model dependent tensor function. The tensor function used to characterize the viscoelastic stress was the White-Metzner model. The form of this model is :

$$\mathbf{T}_1 + I(\dot{\mathbf{g}}, T)\overset{\nabla}{\mathbf{T}}_1 = 2\mathbf{h}_1(\dot{\mathbf{g}})\mathbf{D} \quad [7]$$

$$\mathbf{T}_2 = 2\mathbf{h}_2(\dot{\mathbf{g}})\mathbf{D} \quad [8]$$

where $\overset{\nabla}{\mathbf{T}}_1$ is upper convected derivative of the extra-stress defined by [CRO 82]:

$$\overset{\nabla}{\mathbf{T}}_1 = \frac{D\mathbf{T}_1}{Dt} - \mathbf{T}_1 \cdot \nabla \mathbf{v} + \nabla \mathbf{v}^T \cdot \mathbf{T}_1 \quad [9]$$

5. Boundary and Initial Conditions

The boundary conditions for fluid dynamics on the flow domain $\partial\Omega$ were specified as either velocity components or surface traction components:

$$\mathbf{v} = \bar{\mathbf{v}}(\mathbf{x}, t) \quad \text{for} \quad x \in \partial\Omega_v \quad \text{and} \quad \mathbf{s} \cdot \mathbf{n} = \bar{\mathbf{t}}(\mathbf{x}, t) \quad \text{for} \quad x \in \partial\Omega_t \quad [10]$$

where \mathbf{n} is the outward unit normal to the boundary, and $\bar{\mathbf{v}}$ and $\bar{\mathbf{t}}$ are specified functions. The conditions at the glass mold interface were described as Robin type boundary conditions, where frictional slip is allowed:

$$(\mathbf{s} \cdot \mathbf{n})_t = a(\mathbf{v} - \mathbf{v}^w)_t^b \quad [11]$$

where the subscript refers to the component tangential to the boundary, \mathbf{v}^w is the boundary (or wall) velocity, and a , b are material constants describing the fluid-wall interactions. These constants were determined experimentally using an instrumented plunger that allowed for the determination of the frictional force during pressing.

Thermally, a temperature or heat flux must be specified at the boundaries:

$$T = \bar{T}(x, t) \quad \text{for} \quad x \in \partial\Omega_T \quad \text{and} \quad k(T)\frac{dT}{dn} = \bar{q}_n(\mathbf{x}, t) + q_c + q_r \quad \text{for} \quad x \in \partial\Omega_q \quad [12]$$

where d/dn is the derivative normal to the boundary, \bar{q}_n and \bar{T} are given functions. The quantities q_c and q_r denote the convective and radiative components of the heat flux..

During glass/mold contact the primary mode of heat transfer is contact conductance. In general, the convective heat transfer deviates from perfect contact due to a resistance between the glass and mold. This contact resistance is a thin gas layer consisting of air and combustion products of the lubricant. The gas gap is due to micrononuniformities of the mold surface, thermal contraction of parison, and changes in glass pressure due to pressing/blowing. Expressions for the latter two effects have been previously derived by Pchelyakov and Guloyan [PCH 85]. The gap thickness is determined at each step in the simulation from the local glass temperature distribution and pressure.

6. Free Surface

The position of moving boundaries is determined by solving a kinematic equation:

$$\mathbf{v} \cdot \mathbf{n} = \frac{\partial}{\partial t} \psi(\mathbf{x}_0, t) \cdot \mathbf{n} \quad [13]$$

where \mathbf{n} is the normal to the free surface described by $\psi(\mathbf{x}_0, t)$, and \mathbf{v} is the velocity field evaluated at the free surface. The dynamic condition requires that the normal force be prescribed as either zero or a known value (e.g. blowing). Surface tension enters the system as a force that has the direction normal to the free surface. This is used as a Neumann boundary condition in the momentum equation.

7. Material Properties

In addition to the viscosity of glass discussed above, the glass density, specific heat, radiative, and surface tension properties need to be specified. The glass density was assumed to be constant with a value of 2540 kg/m^3 . The glass surface tension was determined through sessile drop testing completed by the Center for Glass Research at Alfred University. The equation developed by Sharp and Ginther [SHA 51] provides a good estimate for the glass specific heat for a given glass composition.

The heat transfer at high temperatures is determined from both thermal conduction and radiation within the glass. Radiation effects are taken into account as being part of an effective conductivity of the glass. The representation of thermal conductivity in the model is based on the work of Chui and Gardon [CHU 69]. The amount of error introduced by using a diffusion approximation for the glass radiation is not expected to be large except during the inverted reheat and reheat/stretch. During glass/mold contact, the heat flux to the mold/plunger due to semi-transparent radiation is on average an order of magnitude less than that due to contact conductance [STO 98].

8. Numerical Solution

The governing conservation and constitutive equations were solved along with the appropriate boundary conditions using the FEM code POLYFLOW. All models are three-dimensional. To account for the movement of the free surfaces during forming, remeshing techniques were required. Three types of remeshing were used through the

modeling process. The first was simple Lagrangian remeshing where the nodes followed the displacements of the material points. This method was used during gob transfer, parison invert and final blow. During gob formation, inverted reheat, reheat/stretch and parison pressing, the Thompson transformation remeshing technique [THO 85] was used. Unlike standard algebraic remeshing techniques, this method is based on the resolution of a partial differential of the elliptic type, and remains robust for large mesh deformations. The final remeshing technique used involved the exporting of the geometry and remeshing the domain external to POLYFLOW. This was required when the mesh became too distorted or the time steps became too small to continue.

An implicit Euler method was used as the corrector in the time-integration procedure. The time steps were determined from conversion, precision, and contact accuracy requirements set for the problem. Contact was implemented through a standard penalty technique.

9. Results

Figure 1 shows an example of the gob forming process. In the feeder model, the tube rotates and the plungers reciprocate above two orifices. A mesh superposition technique was used in this model. This allowed the mesh of the plungers and glass domains to overlap. The Navier-Stokes and energy equations were modified such that an “inside” flow field was defined where the elements or nodes were assumed to be inside the plungers. Additionally, the mass conservation was modified in order to avoid pressure modes associated with the locking of elements defined inside the plungers.

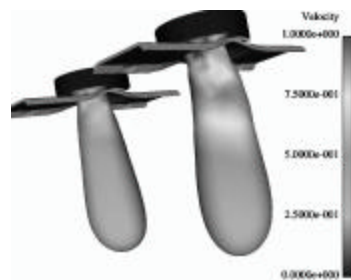


Figure 2: Gob Formation

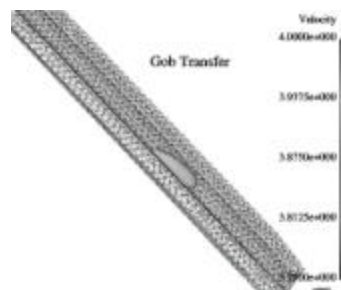


Figure 3: Gob Transfer

The gobs were then allowed to fall through the gob interceptors, on to the scoops, troughs, deflectors, and into the blank (Figure 2). Heat transfer between the gobs and the transfer equipment was modeled using the contact conductance model described above. The temperature of the transfer equipment was measured experimentally.

The next step in the forming process is the pressing of the parison. Several ancillary models are associated with the actual pressing model. Blank mold/neckring and plunger cooling models were developed using FLUENT/UNS. An iterative process was used to determine the operating conditions of the mold and plunger. The heat flux computed from the glass to the mold and plunger in POLYFLOW were cyclically imposed on the mold and plunger in the FLUENT model until an equilibrium condition was met. The forming simulation was then run again with the new mold and plunger temperature distributions. This process was continued until the operating temperatures of the mold

and plunger did not change. Figure 3 shows a cross-section of the parison as it is being pressed. Figure 4 shows a comparison between the glass to mold heat flux determined numerically and a curve based on experimental measurements.

After pressing and a small amount of inverted reheat, the parison is inverted to the blow mold for final blowing. The parison then stretches/reheats and is finally blown into its final shape (see Figure 5). The reheat/final blow model is also an iterative, coupled POLYFLOW/FLUENT simulation. Axial cooling of the blow mold is included, along with vacuum assist effects.

The glass forming physics and ancillary equipment cooling in each of these processes are simulated with advanced numerical tools. A comprehensive approach was used to provide a complete picture of the formation of glass containers process. By modeling all forming processes, insight into the impacts of the various stages in the IS machine on final container quality can be gained. These insights can be used to develop new equipment, and control/cooling schemes for increased production and pack rates.

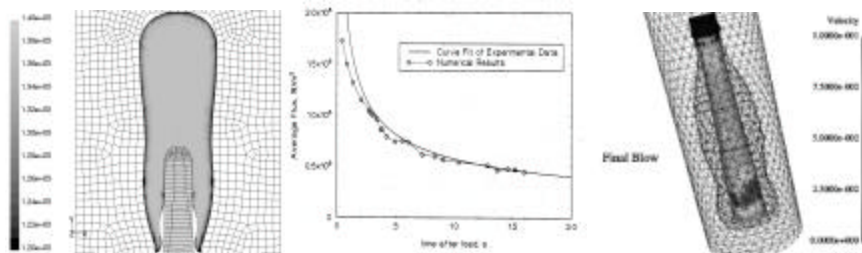


Figure 3: Parison Press Figure 4: Flux Validation Figure 5: Final Blow

10. References

- [CRO 82] CROCHET, M.J. "Numerical Simulation of Die-Entry and Die-Exit Flow of a Viscoelastic Fluid," in Numerical Methods in Industrial Forming Processes, Pineridge Press, 1982.
- [SIM 82] SIMMONS, J.H., MOHR, R.K. AND MONTROSE, C.J., "Non-Newtonian Viscous Flow in Glass", J. Appl. Phys., 53, 4075-4080, 1982.
- [SIM 88] SIMMONS, J.H., OCHOA, R., AND SIMMONS, K.D., "Non-Newtonian Viscous Flow in Soda-Lime-Silica Glass at Forming and Annealing Temperatures," J. of Non-Crystalline Solids, 105, 313-322, 1988.
- [SIM 89] SIMMONS, J.H., SIMMONS, C.J., "Nonlinear Viscous Flow in Glass Forming," Cer. Bull., 66, 1949-1960, 1989.
- [WIL 55] WILLIAMS, M.L., LANDEL, R.F. AND FERRY J.D., The Temperature Dependence of Relaxation Mechanisms in Amorphous Polymers and other Glass-Forming Liquids, J. Am. Chem. Soc., 77, 3701-3706, 1955.
- [PCH 85] PCHELYAKOV, S.K., AND GULOYAN, Y.A., "Heat Transfer at the Glass Mold Interface," Steko i Keramika, 9, 14-15, 1985.
- [SHA 51] SHARP, D.E. AND GINTHER, L.B., "Effect of Composition and Temperature on the Specific Heat of Glass," J. Am. Cer. Soc., 34, 260-271, 1951.
- [CHU 69] CHUI, G.K. AND GARDON, R., "Interaction of Radiation and Conduction in Glass, J. Am. Cer. Soc., 52, 548-553, 1969.
- [THO 85] THOMPSON, J.F., Numerical Grid Generation, Elsevier, 1985.
- [STO 98] STORCK, K., LOYD, D., AND AUGUSTSSON, B., "Heat Transfer Modelling of the Parison Forming in Glass Manufacturing," Glass Technol., 39, 210-216, 1998.